

Evaluating Qubit Control Performance by Indices of Quantum Entanglement

Ciann-Dong Yang, Chin-Wei Chaung and Chung-Hsuan Kuo

Institute of Aeronautics and Astronautics, National Cheng Kung University, Tainan 70101, Taiwan

Abstract: Entangled states are crucial to quantum computation and quantum communication, and are usually treated as the target states to be accessed by quantum control methods. While most of the researches focus on the generation of the desired entangled state at the terminal state $|\psi_f\rangle$, this paper considers the time-varying entanglement of the transient state $|\psi(t)\rangle$ throughout the qubit transfer process. It is found that the degree of entanglement of $|\psi(t)\rangle$ determines how fast and accurately the terminal state $|\psi_f\rangle$ can be achieved. Four quantitative indices of entanglement are employed here to evaluate the degree of entanglement of $|\psi(t)\rangle$ and to estimate the qubit control performance resulting from different control gains in the Lyapunov control law. Our results show that increasing the degree of entanglement during the qubit transfer process is helpful to improve the convergence to the target state; however, increasing control gain tends to destroy the entanglement and attenuate the multi-qubit transfer efficiency. The lack of sufficient quantum correlation between some initial state $|\psi_0\rangle$ and terminal state $|\psi_f\rangle$ is the main reason for unavailable qubit transfer between them. For these states, the insertion of an intermediate entangled state $|\psi_s\rangle$ can effectively increase the degree of entanglement and help to realize the qubit transfer $|\psi_0\rangle \rightarrow |\psi_f\rangle$ via the transition process $|\psi_0\rangle \rightarrow |\psi_s\rangle \rightarrow |\psi_f\rangle$.

Keywords: Qubit quantum control, entangled state, index of quantum entanglement.

1. Introduction

Quantum entanglement is a nonlocal property of multi-particle states, which cannot be described by the combination of several single-particle states. Due to its invariant features under the change of distance of separation, entanglement has been widely exploited in various fields of quantum information techniques such as quantum teleportation [1], quantum computation [2], quantum cryptography [3], and quantum dense coding [4]. The key issue in these quantum information techniques is the preparation and preservation of maximally entangled states. Numerous strategies based on quantum feedback control theory [5] have been proposed to drive the system states to the maximally entangled states. To synthesize the quantum feedback control laws, the information of instantaneous quantum states has to be provided either by simulation or by measurement. Quantum Lyapunov

control [6-8] obtains the state information by simulating the evolution of the system and employs the computed states to construct control fields. This design process yields a feedback-designed open-loop quantum control strategy, which has been shown as a simple way to design control fields for quantum state transfer [9] and entanglement generation [10] without measurement.

The other approach to quantum feedback control is based on the continuous measurement and estimation of the quantum states. Depending on the different measurement processes being employed, three types of measurement-based feedback control were developed, i.e., Markovian feedback control [11-13], Bayesian feedback control [14, 15], and weak-measurement feedback control [16], which all have been applied successfully to the problems of qubit transfer and entanglement generation. Measurement-based feedback control is capable of dealing with unknown initial states and unpredictable disturbances, which otherwise cannot be handled by

Corresponding author: Ciann-Dong Yang, Ph.D., professor, research fields: quantum mechanics, aerospace engineering.

quantum Lyapunov control; nevertheless, the measurement on a quantum system will inevitably influence the states and complicate the design of feedback control.

Irrespective of the strategies being used in quantum feedback control, the generation of entangled states has been formulated as a stabilization problem wherein quantum control laws are designed so that the considered quantum system converges asymptotically to the prescribed entangled states as $t \rightarrow \infty$. Although convergence properties and stability conditions under quantum Lyapunov control have been rigorously analyzed, convergence is not the only requirement for entanglement-generation and qubit-transfer problems, since a convergent solution may experience a long transient process before the steady state $|\psi_f\rangle$ is achieved. Recently, an optimal method [17, 18] has been proposed to speed up Lyapunov quantum control by making the Lyapunov function decrease faster.

Instead of the stability and convergence analysis of a terminal entangled state $|\psi_f\rangle$, which has gained significant progress in recent years, here we will focus on the transient entangled states $|\psi(t)\rangle$ and discuss its influence on the qubit transfer performance throughout the transition process from $|\psi_0\rangle$ and to $|\psi_f\rangle$. Qubit transfer within n-qubit systems composed of n spin-coupled electrons will be considered to reveal the dependence of qubit transfer performance on the entanglement of the transient entangled state under Lyapunov quantum control. It is found that achieving a high degree of entanglement of the transient state $|\psi(t)\rangle$ is not less important than generating a terminal entangled state $|\psi_f\rangle$, because the lack of sufficient entanglement of the transient state $|\psi(t)\rangle$ may lead to a very slow convergent rate to the terminal state $|\psi_f\rangle$ and even lead to the divergence of $|\psi_f\rangle$.

The main distinction between multi-electron and single-electron control problems is the phenomenon of spin entanglement between electrons. Spin entanglement is vulnerable to external field and a

strong magnetic field induced by high-gain control tends to destroy the quantum correlation between electrons and hence attenuate the qubit transfer efficiency. On the contrary, for single-spin control system [8] and energy-level control system [17], which are free from entanglement, high-gain control has a positive effect to accelerate transient response and reduce steady-state error of qubit transfer. To examine the influence of quantum control on the intrinsic entanglement developed within a multi-qubit transfer process, several indices of entanglement including radius of Bloch ball based on Schmidt decomposition [19], entanglement entropy [2], relative entanglement entropy [20], concurrence [21], and entanglement of formation [22], are employed here to quantify the entanglement of the time-varying state $|\psi(t)\rangle$ during the qubit transfer from $|\psi_0\rangle$ to $|\psi_f\rangle$. Based on the evaluation of these indices of entanglement, especially the quantum relative entropy, we find that a strong control field induced by high-gain control blockages the information exchange between electrons, deteriorates their entanglement, and consequently causes the degradation of the qubit transfer performance.

Apart from causing a slow convergent rate, the lack of entanglement in the transient state $|\psi(t)\rangle$ may even render the terminal state inaccessible under quantum control. In order to guarantee the convergence to an arbitrarily assigned target state $|\psi_f\rangle$ under Lyapunov control, the quantum system has to satisfy some prerequisite conditions [9, 23, 24]. Systems not satisfying these convergent conditions are called non-ideal systems, whose convergence to the target state $|\psi_f\rangle$ is solved instead by introducing a series of implicit function perturbations and choosing an implicit Lyapunov function [25, 26]. From the viewpoint of the present paper, the lack of sufficient quantum correlation between the initial and final states is the major reason for unavailable transfer between them. Our analysis gives an alternative approach to improve the convergence to the target

state by increasing the degree of entanglement during the qubit transfer process. This can be done by inserting an intermediate entangled state $|\psi_s\rangle$ into a transition process from $|\psi_0\rangle$ to $|\psi_f\rangle$, between which direct transfer is not possible. The intermediate entangled state $|\psi_s\rangle$ plays the role of an information medium via which information can be exchanged between $|\psi_0\rangle$ and $|\psi_f\rangle$ so that the correlation between them is strengthened to facilitate the qubit transfer $|\psi_0\rangle \rightarrow |\psi_s\rangle \rightarrow |\psi_f\rangle$.

This paper is organized as follows. In Section 2, we express Schrödinger equation and Liouville equation in state-space forms to describe the spin-coupled motion of n electrons. In Section 3, we apply Lyapunov quantum control to realize qubit transfer based on the developed n -spin model. In Section 4, we point out the quantum phenomenon that high-gain Lyapunov control tends to suppress the entanglement between the electrons and attenuate the qubit transfer efficiency. To explain the cause of high-gain degradation, we propose four quantitative indices of entanglement in Section 5 to evaluate the qubit transfer performance, and discuss the dependence of the qubit transfer performance on the degree of spin entanglement between electrons. According to the entanglement-dependent qubit transfer performance, we propose in Section 6 an alternative approach to qubit transfer between two states, for which direct transfer is not possible, by inserting an intermediate entangled state between them. Conclusions are presented in Section 7.

2. Schrödinger and Liouville Equations in State-Space Forms

In this paper, we consider qubit-transfer control of a n -qubit system constituted by n spin-coupled electrons, whose spin motions are described by a n -dimensional complex vector $|\psi(t)\rangle$ and are controlled by an externally applied magnetic field with three components u_x, u_y, u_z . The control field is coupled to the system via time-independent interaction

Hamiltonians $\hat{H}_k, k = x, y, z$. The controlled n -qubit system evolves according to the Schrödinger equation (in dimensionless form)

$$i \frac{d}{dt} |\psi(t)\rangle = \hat{H} |\psi(t)\rangle = \left(\hat{H}_0 + \sum_{k=x,y,z} \hat{H}_k u_k(t) \right) |\psi(t)\rangle \quad (2.1)$$

where \hat{H}_0 is the free Hamiltonian, and $u_k = B_k$ is the k th component of the applied magnetic field $\vec{B} = B_x \vec{e}_x + B_y \vec{e}_y + B_z \vec{e}_z$. The free Hamiltonian \hat{H}_0 considers the spin-coupling energy between neighboring electrons,

$$\hat{H}_0 = \sum_{k=x,y,z} \sum_{i=1}^{n-1} J_{i,i+1} \hat{S}_{i,k} \hat{S}_{i+1,k} \quad (2.2)$$

where $J_{i,i+1}$ is the coupling constant between i th and $(i+1)$ th electrons and $\vec{S}_i = \hat{S}_{i,x} \vec{e}_x + \hat{S}_{i,y} \vec{e}_y + \hat{S}_{i,z} \vec{e}_z$ is the spin vector of the i th electrons. The control Hamiltonian \hat{H}_k considers the interaction between the total spin magnetic moment $\vec{\mu} = \gamma_e \sum_{i=1}^n \vec{S}_i$ and the applied magnetic field \vec{B} . The resulting magnetic potential produced by $\vec{\mu}$ and \vec{B} is given by

$$-\vec{B} \cdot \vec{\mu} = -\gamma_e \vec{B} \cdot \sum_{i=1}^n \vec{S}_i = \sum_{k=x,y,z} \hat{H}_k u_k(t) \quad (2.3)$$

where γ_e is the gyromagnetic ratio of electrons. Accordingly, the control Hamiltonian \hat{H}_k can be expressed as

$$\hat{H}_k = -\gamma_e \sum_{i=1}^n \hat{S}_{i,k}, k = x, y, z \quad (2.4)$$

To express the Schrodinger operator Eq. (2.1) in a state-space form, we note that the vector space of the n -qubit system is spanned by the Zeeman basis

$$|e_k\rangle = |S_1 S_2 \cdots S_n\rangle, k = 1, 2, \dots, 2^n \quad (2.5)$$

where the bit S_i takes the value “0” (spin up) or “1” (spin down), and totally 2^n Zeeman vectors $|e_k\rangle$ can be defined. In terms of $|e_k\rangle$, the n -qubit

state $|\psi(t)\rangle$ can be expanded as

$$|\psi(t)\rangle = x_1|e_1\rangle + x_2|e_2\rangle + \cdots + x_N|e_N\rangle, \quad (2.6)$$

with $N = 2^n$. Under the same basis, the matrix representation of the Hamiltonian operator \hat{H} can be found by the inner product

$$H_{jk} = \langle e_j | \hat{H} | e_k \rangle, j, k = 1, 2, \dots, N \quad (2.7)$$

In conjunction with the vector form of $|\psi(t)\rangle$ and the matrix form of \hat{H} , the state-space expression of the operator Eq. (2.1) turns out to be

$$i \frac{d}{dt} \begin{bmatrix} x_1(t) \\ \vdots \\ x_N(t) \end{bmatrix} = \begin{bmatrix} H_{11} & \cdots & H_{1N} \\ \vdots & \ddots & \vdots \\ H_{N1} & \cdots & H_{NN} \end{bmatrix} \begin{bmatrix} x_1(t) \\ \vdots \\ x_N(t) \end{bmatrix} \quad (2.8)$$

The dimension of the resulting matrix $H \triangleq [H_{jk}]$ is $2^n \times 2^n$, where n is the number of electrons involved in the system. Apparently, as n increases, the element-by-element computation based on Eq. (2.7) becomes very time consuming. An efficient way to compute the matrix $[H_{jk}]$ can be developed by noting the fact that the operators \hat{H}_0 and \hat{H}_k are entirely constituted by the spin operators \hat{S}_x , \hat{S}_y , and \hat{S}_z , whose matrix representations are known as the Pauli matrices

$$\sigma_x = \begin{bmatrix} 0 & 1 \\ 1 & 0 \end{bmatrix}, \sigma_y = \begin{bmatrix} 0 & -i \\ i & 0 \end{bmatrix}, \sigma_z = \begin{bmatrix} 1 & 0 \\ 0 & -1 \end{bmatrix} \quad (2.9)$$

By replacing the spin operator $\hat{S}_{i,k}$ with the Pauli matrix σ_k in Eqs. (2.2) and (2.4), the matrix representation of \hat{H}_0 and $\hat{H}_k, k = x, y, z$, can be obtained at one stroke as

$$H_0 = \sum_{k=x,y,z} \sum_{i=1}^{n-1} J_{i,i+1} I_2 \otimes \cdots \otimes I_2 \otimes (\sigma_k)_i \otimes (\sigma_k)_{i+1} \otimes I_2 \cdots \otimes I_2 \quad (2.10a)$$

$$H_k = -\gamma_e \sum_{i=1}^n I_2 \otimes \cdots \otimes I_2 \otimes (\sigma_k)_i \otimes I_2 \cdots \otimes I_2, \quad (2.10b)$$

where I_2 is the 2×2 identity matrix and the subscript i of $(\sigma_k)_i$ denotes that the Pauli matrix σ_k locates at the i th entry of the sequence of tensor

products in Eq. (2.10). The substitution of the vector representation of $|\psi(t)\rangle$ given by Eq. (2.6) and the matrix representation of \hat{H}_0 and \hat{H}_k given by Eq. (2.10) into Eq. (2.1) yields the bilinear state-space realization of the Schrödinger equation as

$$\dot{x} = -i(H_0 + H_x u_x + H_y u_y + H_z u_z)x, \quad (2.11)$$

The remaining task is to design the control field u_k to drive x to the target state x_f . However, Schrödinger Eq. (2.11) is valid only for the evolution of pure states. Mixed states are otherwise described by the density operator $\hat{\rho} = \sum_j p_j |\psi_j\rangle\langle\psi_j|$, where p_j is the probability of measuring the pure state $|\psi_j\rangle$ from the mixture. The time evolution of the density operator $\hat{\rho}(t)$ is governed by the quantum Liouville equation (in dimensionless form)

$$i \frac{d\hat{\rho}}{dt} = [\hat{H}(t), \hat{\rho}] \triangleq \hat{H}(t)\hat{\rho} - \hat{\rho}\hat{H}(t) \quad (2.12)$$

If there is only one state in the mixture, then quantum Liouville Eq. (2.12) reduces to Schrödinger Eq. (2.1).

To facilitate qubit control involving mixed states, a reformulation of the quantum Liouville equation into an equivalent state-space equation is necessary. This reformulation can be accomplished by transforming Eq. (2.12) from Hilbert space to Liouville space. For every linear operator \hat{A} in the N -dimensional Hilbert space, we can define a vector $|A\rangle\rangle$ in the N^2 -dimensional Liouville space via the relation

$$\hat{A} = \sum_{ij} A_{ij} |e_i\rangle\langle e_j| \leftrightarrow |A\rangle\rangle = \sum_{ij} A_{ij} |ij\rangle\rangle \quad (2.13)$$

where, A_{ij} is the matrix element of \hat{A} under the Zeeman basis, and $|ij\rangle\rangle, i, j = 1, 2, \dots, N$ are the bases of the Liouville vector space. In terms of the Liouville vector $|\rho\rangle\rangle$, we can express the quantum Liouville Eq. (2.12) in a vector form as

$$i \frac{d}{dt} |\rho\rangle\rangle = \hat{\mathcal{L}}(t) |\rho\rangle\rangle \quad (2.14)$$

where $\hat{\mathcal{L}}(t)$ is the Liouville operator defined via the following relation:

$$\hat{\mathcal{L}}(t) |\rho\rangle\rangle \leftrightarrow [\hat{H}(t), \hat{\rho}] \quad (2.15)$$

Once the Liouville operator $\hat{\mathcal{L}}(t)$ has been identified, the quantum Liouville equation can be solved efficiently as the Schrödinger equation. However, till now no general expression for $\hat{\mathcal{L}}(t)$ is available. Here we give an explicit characterization of the Liouville operator $\hat{\mathcal{L}}(t)$ in terms of the Hamiltonian H given by Eq. (2.8) in the 2^n -dimensional Hilbert space. This characterization can be derived by mathematical induction. We begin with the simplest case $n = 1$ involving a single qubit, for which the density operator $\hat{\rho}$, the density matrix ρ , and the Liouville density vector $|\rho\rangle\rangle$ are related by

$$\hat{\rho} \rightarrow \rho = \begin{bmatrix} \rho_{11} & \rho_{12} \\ \rho_{21} & \rho_{22} \end{bmatrix} \rightarrow |\rho\rangle\rangle = \begin{bmatrix} \rho_{11} \\ \rho_{21} \\ \rho_{12} \\ \rho_{22} \end{bmatrix} \quad (2.16)$$

For the case of $n = 1$, an explicit expansion of Eq. (2.14) is given by

$$i \frac{d}{dt} \begin{bmatrix} \rho_{11} \\ \rho_{21} \\ \rho_{12} \\ \rho_{22} \end{bmatrix} = \mathcal{L}(t) \begin{bmatrix} \rho_{11} \\ \rho_{21} \\ \rho_{12} \\ \rho_{22} \end{bmatrix} \quad (2.17)$$

where $\mathcal{L}(t)$ is the 4×4 matrix representation of the Liouville operator $\hat{\mathcal{L}}$. To find the matrix $\mathcal{L}(t)$, we note that Eq. (2.17) is equivalent to Eq. (2.12), which has a matrix representation as

$$\begin{aligned} i \frac{d}{dt} \begin{bmatrix} \rho_{11} & \rho_{12} \\ \rho_{21} & \rho_{22} \end{bmatrix} &= [H(t), \rho(t)] = \begin{bmatrix} H_{11} & H_{12} \\ H_{21} & H_{22} \end{bmatrix} \begin{bmatrix} \rho_{11} & \rho_{12} \\ \rho_{21} & \rho_{22} \end{bmatrix} - \begin{bmatrix} \rho_{11} & \rho_{12} \\ \rho_{21} & \rho_{22} \end{bmatrix} \begin{bmatrix} H_{11} & H_{12} \\ H_{21} & H_{22} \end{bmatrix} \\ &= \begin{bmatrix} H_{12}\rho_{21} - \rho_{12}H_{21} & (H_{11} - H_{22})\rho_{12} + H_{12}\rho_{22} - \rho_{11}H_{12} \\ H_{21}\rho_{11} + (H_{22} - H_{11})\rho_{21} - \rho_{22}H_{21} & H_{21}\rho_{12} - \rho_{21}H_{12} \end{bmatrix} \end{aligned} \quad (2.18)$$

Expressing both sides of the above equation in the form of Liouville vectors, we obtain

$$i \frac{d}{dt} \begin{bmatrix} \rho_{11} \\ \rho_{21} \\ \rho_{12} \\ \rho_{22} \end{bmatrix} = \begin{bmatrix} H_{12}\rho_{21} - H_{21}\rho_{12} \\ H_{21}\rho_{11} + (H_{22} - H_{11})\rho_{21} - \rho_{22}H_{21} \\ -H_{12}\rho_{11} + (H_{11} - H_{22})\rho_{12} + H_{12}\rho_{22} \\ -H_{12}\rho_{21} + H_{21}\rho_{12} \end{bmatrix} \quad (2.19)$$

The equality of Eq. (2.19) with Eq. (2.17) gives

$$\begin{bmatrix} H_{12}\rho_{21} - H_{21}\rho_{12} \\ H_{21}\rho_{11} + (H_{22} - H_{11})\rho_{21} - H_{21}\rho_{22} \\ -H_{12}\rho_{11} + (H_{11} - H_{22})\rho_{12} + H_{12}\rho_{22} \\ -H_{12}\rho_{21} + H_{21}\rho_{12} \end{bmatrix} = \mathcal{L}(t) \begin{bmatrix} \rho_{11} \\ \rho_{21} \\ \rho_{12} \\ \rho_{22} \end{bmatrix} \quad (2.20)$$

from which the Liouville matrix $\mathcal{L}(t)$ can be solved as

$$\begin{aligned} \mathcal{L}(t) &= \begin{bmatrix} 0 & H_{12} & -H_{21} & 0 \\ H_{21} & (H_{22} - H_{11}) & 0 & -H_{21} \\ -H_{12} & 0 & (H_{11} - H_{22}) & H_{12} \\ 0 & -H_{12} & H_{21} & 0 \end{bmatrix} \\ &= \begin{bmatrix} H_{11} & H_{12} & 0 & 0 \\ H_{21} & H_{22} & 0 & 0 \\ 0 & 0 & H_{11} & H_{12} \\ 0 & 0 & H_{21} & H_{22} \end{bmatrix} - \begin{bmatrix} H_{11} & 0 & H_{21} & 0 \\ 0 & H_{11} & 0 & H_{21} \\ H_{12} & 0 & H_{22} & 0 \\ 0 & H_{12} & 0 & H_{22} \end{bmatrix} \\ &= \begin{bmatrix} 1 & 0 \\ 0 & 1 \end{bmatrix} \otimes \begin{bmatrix} H_{11} & H_{12} \\ H_{21} & H_{22} \end{bmatrix} - \begin{bmatrix} H_{11} & H_{21} \\ H_{12} & H_{22} \end{bmatrix} \otimes \begin{bmatrix} 1 & 0 \\ 0 & 1 \end{bmatrix} = I_2 \otimes H - H^T \otimes I_2 \end{aligned} \quad (2.21)$$

Above Liouville matrix for a single qubit can be generalized directly to the n-qubit case as

$$\mathcal{L}(t) = I_{2^n} \otimes H - H^T \otimes I_{2^n} \quad (2.22)$$

where $H = H_0 + \sum_{k=x,y,z} H_k u_k$ is the n-qubit Hamiltonian with H_0 and H_k given by Eq. (2.10).

The validity of Eq. (2.22) can be proved by mathematical induction by assuming firstly that Eq. (2.22) is satisfied for $n > 1$ and then showing its validity for $n + 1$. With $\mathcal{L}(t)$ given by Eq. (2.22), the state-space representation of the quantum Liouville Eq. (2.14) becomes

$$i \frac{d}{dt} |\rho\rangle\rangle = (I_{2^n} \otimes H - H^T \otimes I_{2^n}) |\rho\rangle\rangle \quad (2.23)$$

where, H is a $2^n \times 2^n$ matrix and $|\rho\rangle\rangle$ is a 2^{2n} -dimensional vector. Eq. (2.23) can be applied to the qubit-transfer control for both pure states and mixed states and can be solved as efficient as the state-space Schrödinger Eq. (2.11).

3. Qubit Transfer by Lyapunov Control

The quantum model provided by Eqs. (2.11) and (2.23) will be employed in this section to investigate the role of entanglement in the qubit transfer from an initial state $|\psi_0\rangle$ to a terminal state $|\psi_f\rangle$ for pure state transfer, or from an initial density matrix ρ_0 to a terminal density matrix ρ_f for mixed states. Among a variety of quantum control methodologies, Lyapunov quantum control will be adopted here to achieve the prescribed qubit transfer for its clarity of demonstration. The strategy of the Lyapunov control is simply to make the first-order time derivative of a chosen Lyapunov function non-positive. Three types of Lyapunov functions, respectively, based on state distance, state error, and the average value of a mechanical quantity have been proposed in the literature [6]. Being a generalization of the first two types, the Lyapunov function based on the average value of a mechanical quantity P assumes the following form

$$V(\psi) = \langle \psi | \hat{P} | \psi \rangle = \text{Trace}(\hat{P} \hat{\rho}) \quad (3.1)$$

where \hat{P} is the Hermitian operator associated with the observable P and $\text{Trace}(\hat{P} \hat{\rho})$ represents the average value of this mechanical quantity in the state $|\psi\rangle$. With a proper choice of \hat{P} , the Lyapunov function given by Eq. (3.1) turns out to be a measure of the state distance or the state error between $|\psi(t)\rangle$ and $|\psi_f\rangle$. While $V(\psi)$ approaches to its minimum

$$\begin{aligned} \dot{V}(\rho') &= \text{Trace}(P \dot{\rho}') \\ &= \text{Trace} \left(P \sum_{k=x,y,z} A_k(t) u_k(t) \rho'(t) - P \sum_{k=x,y,z} \rho'(t) A_k(t) u_k(t) \right) \\ &= \sum_{k=x,y,z} u_k(t) \cdot \text{Trace}([\rho'(t), P] A_k(t)) \end{aligned} \quad (3.4)$$

value according to the control strategy $\dot{V} \leq 0$, the quantum state $|\psi\rangle$ will converge to the desired target state $|\psi_f\rangle$ if the operator \hat{P} is chosen in such a way that the target state $|\psi_f\rangle$ is the eigenvector of \hat{P} corresponding to the minimum eigenvalue. The conditions for ensuring the convergence to an arbitrarily assigned target state $|\psi_f\rangle$ under Lyapunov control have been investigated elaborately in the literature. Here we will focus on the transient response of Lyapunov quantum control and discuss the influence of spin entanglement on the qubit transfer performance during the transition process.

The design of Lyapunov control law is rather straightforward, which starts with the application of the following unitary transformation to the density matrix ρ

$$\rho' = e^{iH_0 t/\hbar} \rho e^{-iH_0 t/\hbar} \quad (3.2)$$

where, ρ' is known as the density matrix under the interaction picture [8]. The transformed quantum Liouville equation becomes homogenous in the form of

$$\frac{d}{dt} \rho'^{(t)} = [H'^{(t)}, \rho'^{(t)}] = \left[\sum_{k=x,y,z} A_k(t) u_k(t), \rho'^{(t)} \right] \quad (3.3)$$

with $A_k(t) = -ie^{iH_0 t} H_k e^{-iH_0 t}$. Since the unitary transformation does not change the distribution of the qubit populations, Lyapunov control law can be designed directly under the interaction picture. It can be seen that the transformed Eq. (3.3) removes the constant term H_0 and retains only the bilinear terms involving u_k and ρ' . The resulting model simplifies the problem of designing the control law to meet the requirement $\dot{V} \leq 0$. Based on Eq. (3.1), the Lyapunov function can be chosen as $V(\rho') = \text{Trace}(P \rho')$, whose time derivative appears to be

To ensure the satisfaction of the condition $\dot{V}(\rho') \leq 0$, the simplest control law takes the following form

$$u_k(t) = -k_p \cdot \text{Trace}([\rho'(t), P]A_k(t)) \quad (3.5)$$

where, $k_p > 0$ is a control gain. The condition $\dot{V}(\rho') \leq 0$ alone cannot guarantee the asymptotic convergence to the target state $|\psi_f\rangle$. The additional condition for asymptotic convergence can be satisfied by choosing the mechanical quantity P in the Lyapunov Eq. (3.1) as

$$P = -\rho_f = -|\psi_f\rangle\langle\psi_f|. \quad (3.6)$$

It can be shown that the above choice of P leads to the following Lyapunov function

$$V(\rho') = \text{Trace}(P\rho') = \langle\psi|P|\psi\rangle = -|\langle\psi|\psi_f\rangle|^2 \quad (3.7)$$

Because the minimum value $V = -1$ occurs at $|\psi\rangle = |\psi_f\rangle$, the condition $\dot{V} \leq 0$ ensures that the quantum state $|\psi\rangle$ is eventually driven to the target state $|\psi_f\rangle$, while the control law of Eq. (3.5) decreases the Lyapunov function V to its minimum value.

With the Lyapunov control law of Eq. (3.5) and the Lyapunov Eq. (3.7), the convergence to the target state $|\psi_f\rangle$ is guaranteed. Our main concern is how to quantify and improve the transient performance of the qubit transfer between $|\psi_0\rangle$ and $|\psi_f\rangle$. For this purpose, several indices of spin entanglement will be

$$H = H_0 + \sum_{k=x,y,z} H_k u_k(t), = J_{1,2} \sum_{k=x,y,z} \sigma_k \otimes \sigma_k - \gamma_e \sum_{k=x,y,z} (\sigma_k \otimes I_2 + I_2 \otimes \sigma_k) u_k(t) \quad (4.2)$$

According to the definition of the Pauli matrices in Eq. (2.9), the Hamiltonians can be expressed explicitly as

$$H_0 = J_{1,2} \begin{bmatrix} 1 & 0 & 0 & 0 \\ 0 & -1 & 2 & 0 \\ 0 & 2 & -1 & 0 \\ 0 & 0 & 0 & 1 \end{bmatrix}, H_x = -\gamma_e \begin{bmatrix} 0 & 1 & 1 & 0 \\ 1 & 0 & 0 & 1 \\ 1 & 0 & 0 & 1 \\ 0 & 1 & 1 & 0 \end{bmatrix} \quad (4.3a)$$

$$H_y = -\gamma_e \begin{bmatrix} 0 & -i & -i & 0 \\ i & 0 & 0 & -i \\ i & 0 & 0 & -i \\ 0 & i & i & 0 \end{bmatrix}, H_z = -\gamma_e \begin{bmatrix} 2 & 0 & 0 & 0 \\ 0 & 0 & 0 & 0 \\ 0 & 0 & 0 & 0 \\ 0 & 0 & 0 & -2 \end{bmatrix} \quad (4.3b)$$

where the coupling constant is set to $J_{1,2} = 1$, and the gyromagnetic ratio of electrons is normalized to $\gamma_e = -1$ in the following numerical demonstrations. With the given Hamiltonian H , the time evolution of

introduced to evaluate the qubit control performance and the control gain k_p in Eq. (3.5) is to be accommodated to improve the control performance in response to the change of spin entanglement during the qubit transfer process.

4. High-Gain Degradation of Qubit Control Efficiency

Quantum entanglement dominates the qubit transfer performance and a well understanding of the influence of quantum control on the degree of entanglement is helpful to the control law design. The simplest entangled system is composed of two spin-coupled electrons, for which several definitions of entanglement have been well developed [27]. The two-electron spin motion can be described by the four bases, $|00\rangle$, $|01\rangle$, $|10\rangle$, and $|11\rangle$, and any two-spin state $|\psi(t)\rangle_{AB}$ of the system can be expressed as a superposition of the four bases:

$$|\psi(t)\rangle_{AB} = x_1(t)|00\rangle + x_2(t)|01\rangle + x_3(t)|10\rangle + x_4(t)|11\rangle \quad (4.1)$$

where, $x_i(t)$, $i = 1, 2, 3, 4$, are time-varying expansion coefficients. The time evolution of $|\psi(t)\rangle_{AB}$ is governed by the Schrodinger Eq. (2.7) with Hamiltonians H_0 and H_k given by Eq. (2.10) for $n = 2$:

the density matrix $\rho(t) = |\psi(t)\rangle\langle\psi(t)|$ is then solved from the quantum Liouville Eq. (2.12) through two sequential transformations $\rho \rightarrow \rho' \rightarrow |\rho''\rangle$. The first one, $\rho \rightarrow \rho'$, is the unitary transformation given

by Eq. (3.2) and the second one, $\rho' \rightarrow |\rho'\rangle\rangle$, is the matrix-to-vector transformation via Eq. (2.13). After the two transformations, the quantum Liouville equation becomes

$$\frac{d}{dt}|\rho'(t)\rangle\rangle_{16 \times 1} = (I_4 \otimes H' - H'^T \otimes I_4)|\rho'(t)\rangle\rangle_{16 \times 1} \quad (4.4)$$

where, $H'(t) = \sum_{k=x,y,z} A_k(t)u_k(t)$ is the transformed Hamiltonian defined in Eq.(3.3) and the magnetic field $u_k(t)$ is synthesized by Eq. (3.5) via Lyapunov control design.

The influence of the control gain k_p on the qubit transfer from $|00\rangle$ to $|11\rangle$ will be studied firstly in order to reveal the dependence of the qubit transfer

performance on the degree of spin entanglement between the two electrons. Under the action of the control law of Eq. (3.5), the qubit populations, i.e., the diagonal elements of $\rho(t)$, are obtained by solving Eq. (4.4) with initial density matrix $\hat{\rho}_0 = |00\rangle\langle 00|$. The numerical results by using four different control gains $k_p = 1, 2, 14, 20$, are shown in Fig. 1. It can be seen that for the low-gain cases $k_p = 1$ and $k_p = 2$, the transition from $|00\rangle$ to $|11\rangle$ is 100% completed within 50 and 35 time units, respectively. For the high-gain cases $k_p = 14$ and $k_p = 20$, the transfer percentage reduces to 90% and 65%, respectively, although high-gain control leads to faster transient response and larger control field as illustrated in Fig. 2.

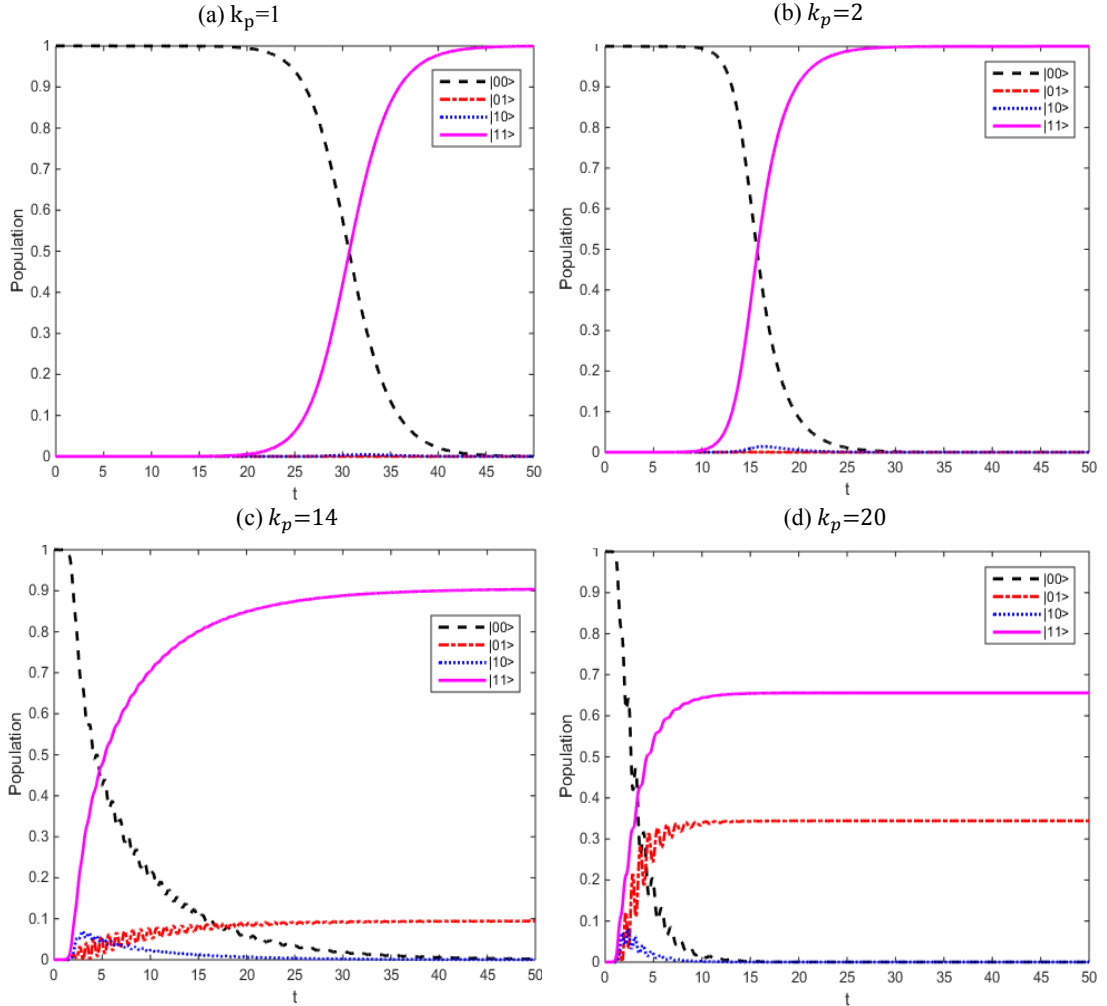


Fig. 1 The time responses of the qubit populations in the two-qubit transfer from $|00\rangle$ to $|11\rangle$ by using four different control gains $k_p = 1, 2, 14, 20$.

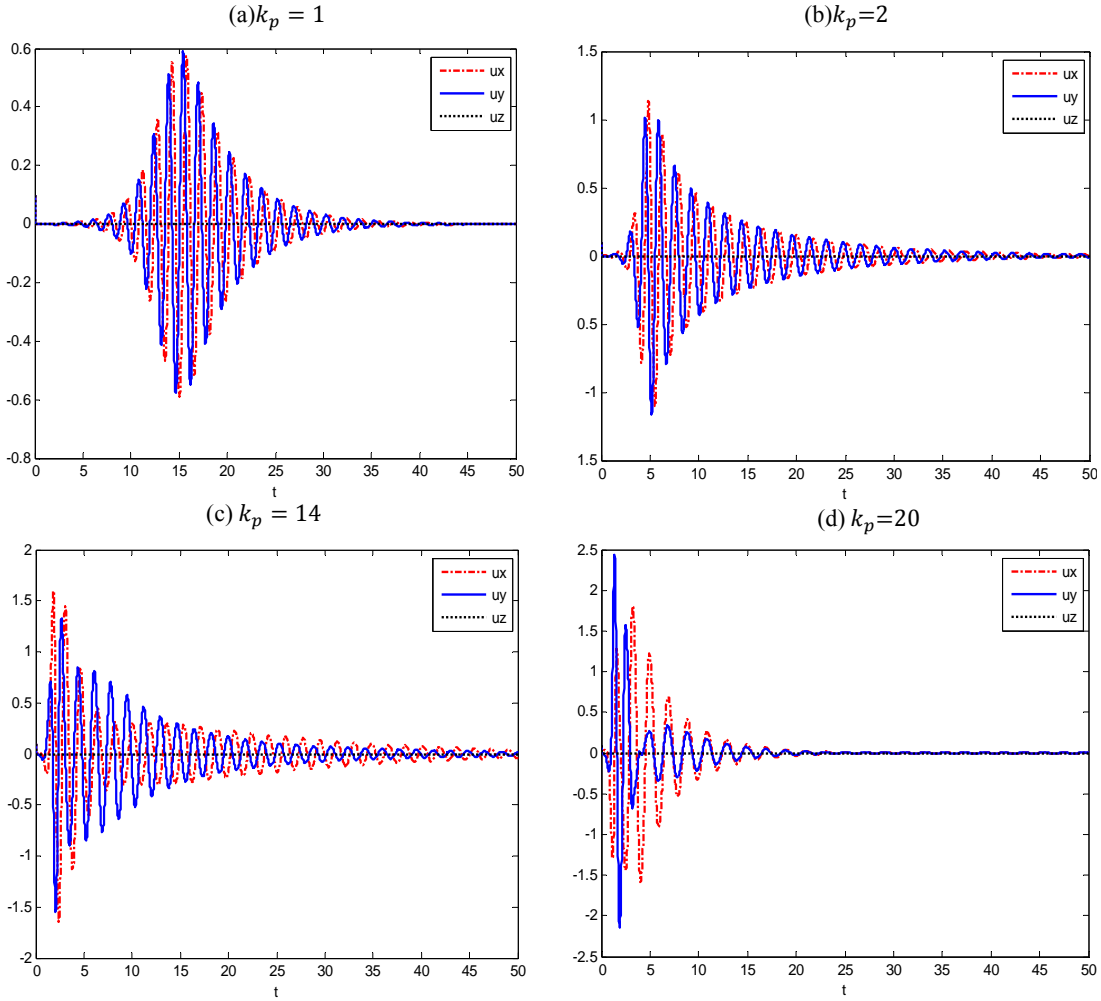


Fig. 2 The applied control field in the two-qubit transfer from $|00\rangle$ to $|11\rangle$ by using four different control gains $k_p = 1, 2, 14, 20$.

If the control gain increases further, the achieved population level begins to oscillate with increasing amplitude, and diverges eventually. This observation is contrary to our common expectation that a high-gain control tends to decrease the steady-state error. Additional computations have been conducted for three- and four-electron systems by solving Eq. (4.4) and similar high-gain degradation of transfer efficiency occurs.

A reasonable explanation to high-gain degradation of multi-qubit transfer performance is that spin entanglement between two electrons is vulnerable to external field and a high-gain control tends to suppress the interconnection between the electrons and hence attenuate the qubit transfer efficiency. To

confirm this conjecture, we employ the same governing Eq. (4.4) and the same control law of Eq. (3.5) to examine whether high-gain degradation takes place in the single-qubit transfer process, where only one electron is involved and no entanglement effect can emerge. In contrast with the two-qubit results, two control gains $k_p = 2$ and $k_p = 20$, which are representative values of low gain and high gain, are applied to the one-qubit transfer from $|0\rangle$ to $|1\rangle$. As shown in Fig. 3, high-gain control of single qubit transfer yields much faster transient response than those by using low-gain control. Moreover, high-gain control simplifies the shape of the control field, while low-gain control produces high-frequency oscillation of the control field, as demonstrated in Figs. 3c and 3d.

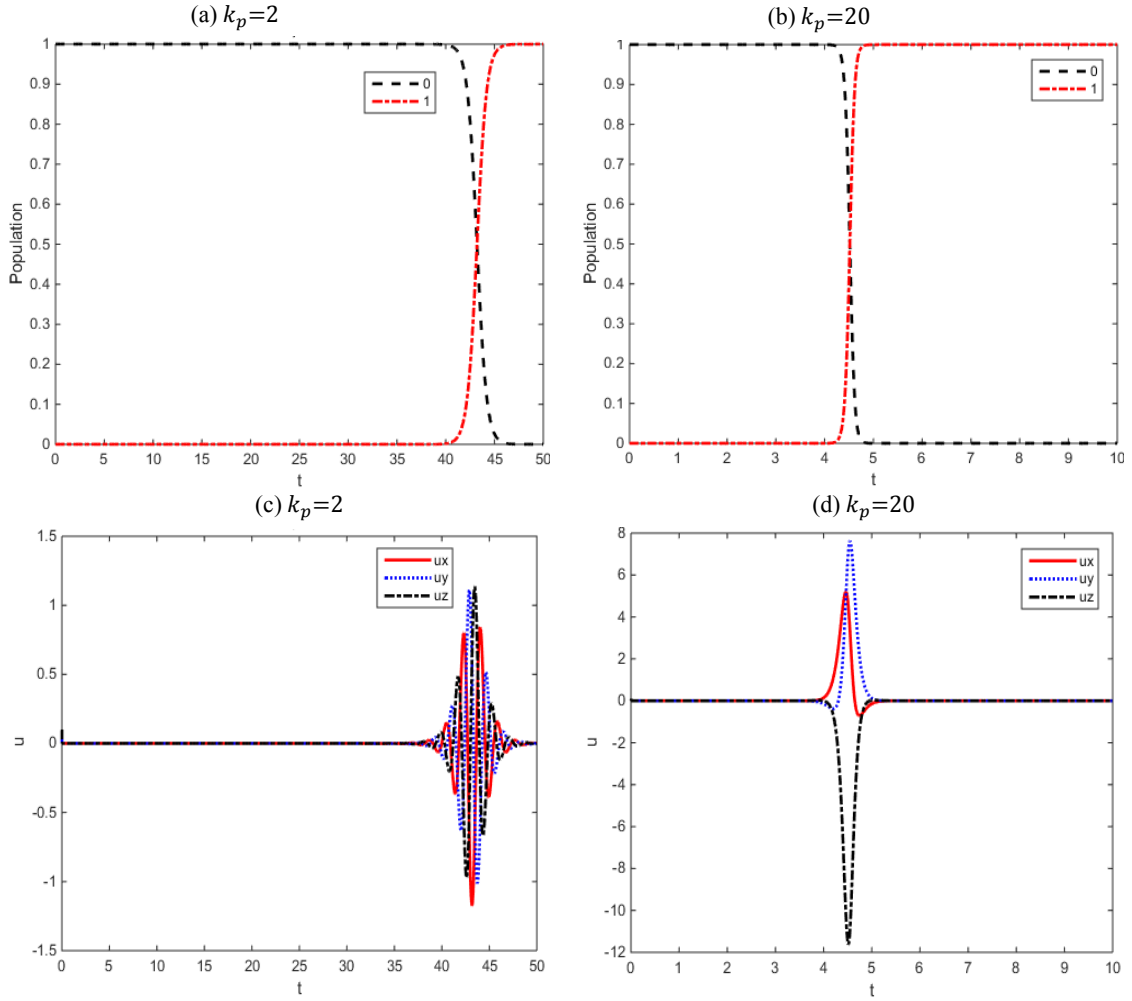


Fig. 3 The time responses of the population and the applied control field for the single qubit transfer from $|0\rangle$ to $|1\rangle$ by using (a) low control gain $k_p = 2$ and (b) high control gain $k_p = 20$.

It appears that contrary to two-qubit transfer, high-gain control is otherwise beneficial to single qubit transfer. To further strengthen this standpoint, we also apply high-gain control to a Morse oscillator with four energy levels, which is free from entanglement. The result is the same as that of single-qubit transfer, indicating that high-gain control inclines to destroy the entanglement between electrons and attenuate the multi-qubit transfer efficiency, but it has no adverse effect on quantum systems free from entanglement.

5. Evaluating Qubit Transfer Performance by Index of Entanglement

Quantum entanglement appears exclusively in

multi-particle systems and plays a dominant role in the performance of multi-qubit transfer control. The appearance of entanglement makes the results of quantum control totally different from those obtained from single-particle systems. The degree of entanglement of the transient state $|\psi(t)\rangle$ determines to show fast and accurate the terminal state $|\psi_f\rangle$ can be achieved. For the purpose of clarifying the role of entanglement in qubit transfer performance, four quantitative indices of entanglement will be employed in this section to evaluate the degree of entanglement of $|\psi(t)\rangle$ and to estimate the qubit control performance resulting from different control gains k_p in the Lyapunov control law of Eq. (3.5).

Firstly, the Schmidt decomposition [19] of the

two-spin quantum system $|\psi\rangle_{AB}$ will be applied to the computation of the indices of entanglement. A two-spin state $|\psi\rangle_{AB}$ is said to be separable, if it can be separated into a product $|\psi\rangle_{AB} = |\psi\rangle_A \otimes |\psi\rangle_B$, where $|\psi\rangle_A \in \mathcal{H}_A$, $|\psi\rangle_B \in \mathcal{H}_B$ with \mathcal{H}_A and \mathcal{H}_B being the Hilbert spaces of the individual electrons; otherwise the state is called an entangled state. With this definition, we will see that in the qubit transfer process considered previously, the transient quantum state $|\psi(t)\rangle_{AB}$ is entangled over the entire process, except for the initial state $|00\rangle_{AB} = |0\rangle_A \otimes |0\rangle_B$ and the terminal state $|11\rangle_{AB} = |1\rangle_A \otimes |1\rangle_B$. The Schmidt decomposition provides us an effective mathematical tool to estimate the degree of quantum entanglement in the transient state $|\psi(t)\rangle_{AB}$.

5.1 Schmidt Decomposition

At any instant t , the transient state $|\psi(t)\rangle_{AB}$ can be expressed as a linear superposition of the four qubits as given by Eq. (4.1). Although the separation $|\psi(t)\rangle_{AB} = |\psi(t)\rangle_A \otimes |\psi(t)\rangle_B$ is not possible for entangled states, the Schmidt decomposition of $|\psi(t)\rangle_{AB}$ always exists and takes the following form

$$|\psi(t)\rangle_{AB} = c_1(t)|u_A(t)\rangle \otimes |u_B(t)\rangle + c_2(t)|v_A(t)\rangle \otimes |v_B(t)\rangle \quad (5.1)$$

where, $c_1(t)$ and $c_2(t)$ are expansion coefficients satisfying $|c_1(t)|^2 + |c_2(t)|^2 = 1$; $|u_A(t)\rangle$ and $|v_A(t)\rangle$ are the unit orthogonal vectors of the Hilbert space \mathcal{H}_A , and $|u_B(t)\rangle$ and $|v_B(t)\rangle$ are the unit orthogonal vectors of the Hilbert space \mathcal{H}_B . At any instant t , the coefficients c_1 and c_2 , and the unit vectors $|u_i(t)\rangle$ and $|v_i(t)\rangle$, $i = A, B$, can be determined uniquely by the expansion coefficients $x_i(t)$ defined in Eq. (4.1). The Schmidt decomposition in Eq. (5.1) offers an analytical expression for the reduced density matrices ρ_A and ρ_B , which can be found from $\rho_{AB} = |\psi(t)\rangle_{AB}\langle\psi(t)|$ according to their definitions:

$$\begin{aligned} \rho_A &= \text{Trace}_B(\rho_{AB}) = |c_1(t)|^2|u_A(t)\rangle\langle u_A(t)| \\ &\quad + |c_2(t)|^2|v_A(t)\rangle\langle v_A(t)| \quad (5.2a) \\ \rho_B &= \text{Trace}_A(\rho_{AB}) = |c_1(t)|^2|u_B(t)\rangle\langle u_B(t)| \\ &\quad + |c_2(t)|^2|v_B(t)\rangle\langle v_B(t)| \quad (5.2b) \end{aligned}$$

Expanding the unit vectors $|u_i(t)\rangle$ and $|v_i(t)\rangle$ with respect to the Zeeman basis $\{|0\rangle, |1\rangle\}$ with expansion coefficients expressed in terms of $x_i(t)$ for each subsystem, we obtain the reduced density matrices for the two electrons, respectively, as

$$\rho_A(t) = \begin{bmatrix} x_1^2 + x_2^2 & x_1x_3^* + x_2x_4^* \\ x_3x_1^* + x_4x_2^* & x_3^2 + x_4^2 \end{bmatrix} \quad (5.3a)$$

$$\rho_B(t) = \begin{bmatrix} x_1^2 + x_3^2 & x_1x_2^* + x_3x_4^* \\ x_2x_1^* + x_4x_3^* & x_2^2 + x_4^2 \end{bmatrix} \quad (5.3b)$$

Because the trajectory representation of spin motion on the Bloch sphere is available only for single electron, the separated expressions for ρ_A and ρ_B obtained by Eq. (5.3) allow us to describe the spin-coupled motion of two electrons on the two separated Bloch spheres. The spin motion of each electron on the Bloch sphere is described by the Bloch vector $\vec{n} = (n_x, n_y, n_z)$, which is connected to the density matrix via the following relation

$$\rho = \frac{1}{2} \begin{bmatrix} 1 + n_z & n_x - in_y \\ n_x + in_y & 1 - n_z \end{bmatrix} \quad (5.4)$$

The comparison between Eqs. (5.3) and (5.4) gives the Bloch vector for each electron in terms of the expansion coefficients $x_i(t)$ as

$$\begin{bmatrix} n_{Ax}(t) \\ n_{Ay}(t) \\ n_{Az}(t) \end{bmatrix} = \begin{bmatrix} x_1x_3^* + x_2x_4^* + x_3x_1^* + x_4x_2^* \\ i(x_1x_3^* + x_2x_4^* - x_3x_1^* - x_4x_2^*) \\ |x_1|^2 + |x_2|^2 - |x_3|^2 - |x_4|^2 \end{bmatrix} \quad (5.5a)$$

$$\begin{bmatrix} n_{Bx}(t) \\ n_{By}(t) \\ n_{Bz}(t) \end{bmatrix} = \begin{bmatrix} x_1x_2^* + x_3x_4^* + x_2x_1^* + x_4x_3^* \\ i(x_1x_2^* + x_3x_4^* - x_2x_1^* - x_4x_3^*) \\ |x_1|^2 + |x_3|^2 - |x_2|^2 - |x_4|^2 \end{bmatrix} \quad (5.5b)$$

The magnitude of the Bloch vector $|\vec{n}(t)|$ forms the radius of the Bloch ball. Regarding the geometrical meaning of the Bloch sphere, we note that when $|\vec{n}(t)| = 1$, the two-spin system is instantaneously in a separable state (non-entangled state), while when $|\vec{n}(t)| < 1$, the two-spin system is in an entangled state and its degree of entanglement increases with decreasing $|\vec{n}(t)|$. As $|\vec{n}(t)|$ decreases to zero, the two-spin system reaches the maximally entangled state. Accordingly, the radius of the Bloch ball derived from the Schmidt

decomposition can be conceived of as a quantitative measure of entanglement and the time response of $|\vec{n}(t)|$ plotted in the spherical coordinate turns out to be a vivid visualization of the time-varying entanglement between the two electrons during a qubit transfer process.

The time response of the Bloch radius $|\vec{n}(t)|$ is computed by substituting the time-varying coefficients $x_i(t)$ obtained from Eq. (2.11) into Eq. (5.5). Fig. 4 plots the results for the two-qubit transfer from $|00\rangle$ to $|11\rangle$ by using the Lyapunov control law of Eq. (3.5) with control gain $k_p = 2$ and $k_p = 20$. It can be seen that except for the initial state and the final state, the radius of the Bloch ball is always smaller than one with its minimum value occurring in the middle of the transition process. This time response of $|\vec{n}(t)|$ manifests that the transient state $|\psi(t)\rangle_{AB}$ is a time-varying entangled state with its degree of entanglement increasing from zero at the initial state $|00\rangle$ to a maximum in the middle of the transition, and then returning back to zero at the terminal state $|11\rangle$. The effect of increasing the control gain k_p is to speed up the transient response of $|\vec{n}(t)|$; however, high-gain control is also found to attenuate and oscillate the entanglement, as shown in Fig. 4b. This

deterioration of entanglement due to high-gain control partially explains the reason why the qubit transfer from $|00\rangle$ to $|11\rangle$ is unsuccessful by using $k_p = 20$ as already shown in Fig. 1d.

5.2 Entanglement Entropy

Qubit transfer involves information exchange among all the possible states participating in the qubit transfer process. The amount of information contained in a mediate entangled state determines the efficiency of the qubit transfer through this entangled state. The von Neumann entropy [2] defined by

$$S(\rho) = -\text{Trace}(\rho \log_2 \rho) \quad (5.6)$$

, which is a useful index to quantify the amount of information contained in a quantum state, or equivalently, the amount of uncertainty before the quantum state is measured. In terms of the Schmidt decomposition of the two-electron state $|\psi(t)\rangle_{AB}$, the entanglement entropy $E(\psi(t))$ of $|\psi(t)\rangle_{AB}$ is equivalent to the von Neumann entropy of its subsystems as

$$\begin{aligned} E(\psi(t)) &= S(\rho_A) = S(\rho_B) \\ &= -|c_1(t)|^2 \log_2 |c_1(t)|^2 - |c_2(t)|^2 \log_2 |c_2(t)|^2 \end{aligned} \quad (5.7)$$

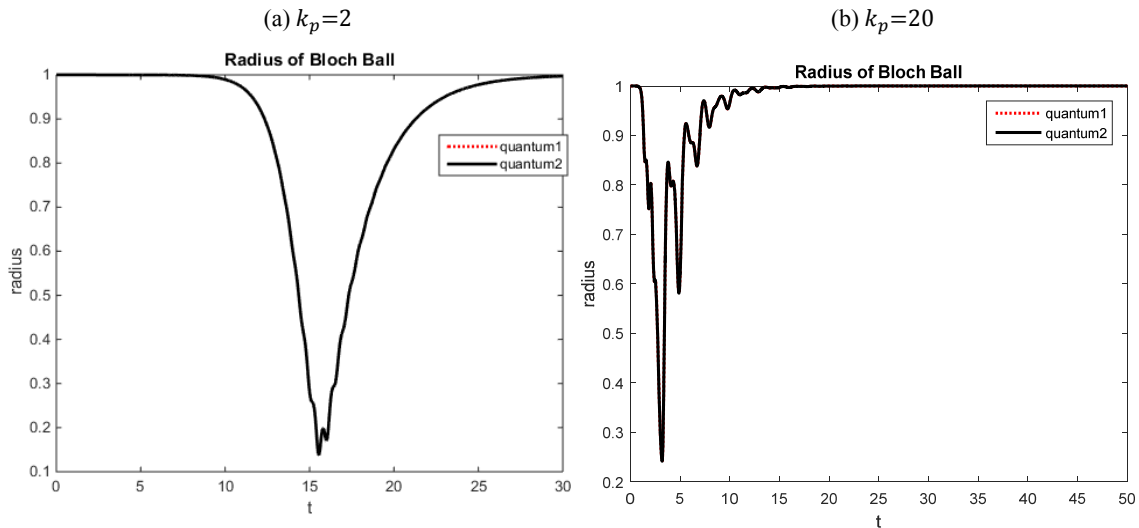


Fig. 4 The time responses of the radius of Bloch ball in the two-qubit transfer from $|00\rangle$ to $|11\rangle$ by using (a) low control gain $k_p = 2$ and (b) high control gain $k_p = 20$.

where $\rho_A(t)$ and $\rho_B(t)$ are given by Eq. (5.3). Due to the equality $|c_1|^2 + |c_2|^2 = 1$, the maximal entanglement entropy $E(\psi(t)) = 1$ occurs at $|c_1|^2 = |c_2|^2 = 1/2$, and the minimum occurs at $c_1 = 0$ or $c_2 = 0$, corresponding to the separable situation. Fig. 5 demonstrates the time history of $E(\psi(t))$ in the qubit transfer process from $|00\rangle$ to $|11\rangle$ with two different control gains $k_p = 2$ and $k_p = 20$. As shown in Fig. 5, the entanglement entropy achieves its maximum in the middle of the transition, where the entangled state contains the maximal amount of information; however, the absolute maximum $E(\psi(t)) = 1$ is not attained using the control law of Eq. (3.5) with the assumed control gains. The comparison between Figs. 4 and 5 reveals the similar tendency of the entanglement entropy $E(\psi(t))$ and the Bloch radius $|\vec{n}(t)|$ in that the occurrence of the relative maximum of $E(\psi(t))$ coincides with the minimum of $|\vec{n}(t)|$. Meanwhile, the attenuation of entanglement due to high-gain control is also reflected in the index of entanglement entropy, whose maximal value decreases from 0.69 to 0.66 as k_p increases from 2 to 20, as depicted in Figs. 5a and 5b.

5.3 Relative Entanglement Entropy

Both the entanglement entropy and the Bloch-ball radius indicate that the high-gain control has no positive effect on increasing the degree of entanglement in a two-electron system. However, these two indices of entanglement are still not strong enough to explain the failure of qubit transfer from $|00\rangle$ to $|11\rangle$ as shown in Fig. 1d. The main damage to entanglement caused by high-gain control is the blockage of information exchange between the electrons. The entanglement entropy and the Bloch-ball radius measure the amount of information contained in individual electrons, but they do not exhibit the amount of information exchange between the two electrons. When more information is exchanged, the quantum states of the two electrons get closer to each other, i.e., more information is shared by the two states.

Quantum relative entropy $S(\rho_A||\rho_B)$ is a useful measure of the closeness between two quantum states ρ_A and ρ_B , which is defined as Ref. [20]

$$\begin{aligned} S(\rho_A||\rho_B) &= \text{Trace}(\rho_A \log_2 \rho_A) \\ &\quad - \text{Trace}(\rho_A \log_2 \rho_B) \\ &= -S(\rho_A) - \text{Trace}(\rho_A \log_2 \rho_B) \end{aligned} \quad (5.8)$$

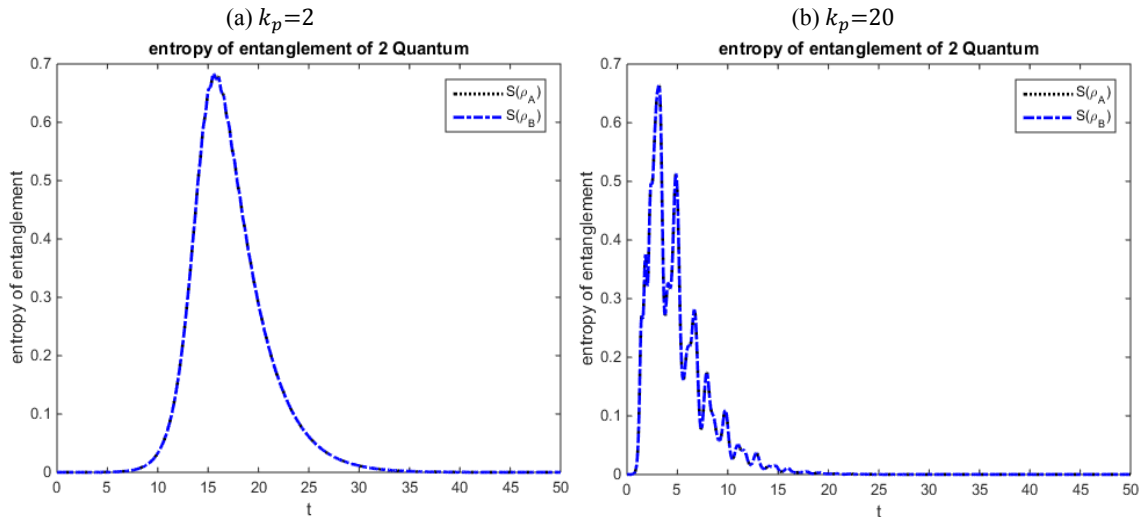


Fig. 5 Time history of the entanglement entropy $E(\psi(t))$ in the qubit transfer process from $|00\rangle$ to $|11\rangle$ with two different control gains $k_p = 2$ and $k_p = 20$.

It quantifies the amount of information, which belongs to ρ_A and at the same time is shared with ρ_B . The value of $S(\rho_A||\rho_B)$ is a non-negative number with minimum $S(\rho_A||\rho_B) = 0$ corresponding to the situation that the information of ρ_A is fully shared with ρ_B , i.e., the distance between ρ_A and ρ_B is zero. The amount of information shared by ρ_A and ρ_B decreases with increasing $S(\rho_A||\rho_B)$. With ρ_A and ρ_B computed by Eq. (5.3), the time responses of the quantum relative entropy $S(\rho_A||\rho_B)$ in the qubit transfer process from $|00\rangle$ to $|11\rangle$ are shown in Fig. 6a with control gain $k_p = 2$. The value of $S(\rho_A||\rho_B)$ keeps smaller than 0.08 over the entire transition process, indicating that the information contained in ρ_A and ρ_B is nearly equivalent. Fig. 6b illustrates

$S(\rho_A||\rho_B)$ as the difference between $S(\rho_A)$ and $-\text{Trace}[\rho_A \log_2 \rho_B]$, showing that the two curves are almost coincident for $k_p = 2$. However, as we increase the control gain to $k_p = 6$, the difference between $S(\rho_A)$ and $-\text{Trace}[\rho_A \log_2 \rho_B]$ becomes significant as shown in Fig. 6c. As k_p increases further to 20, the great discrepancy between $S(\rho_A)$ and $-\text{Trace}[\rho_A \log_2 \rho_B]$ shown in Fig. 6d manifests the loss of information exchange between the two electrons. The quantum relative entropy $S(\rho_A||\rho_B)$ persuasively indicates that a high-gain control blockages the information exchange between the two electrons and causes the degradation of the qubit transfer performance as already shown in Fig. 1d.

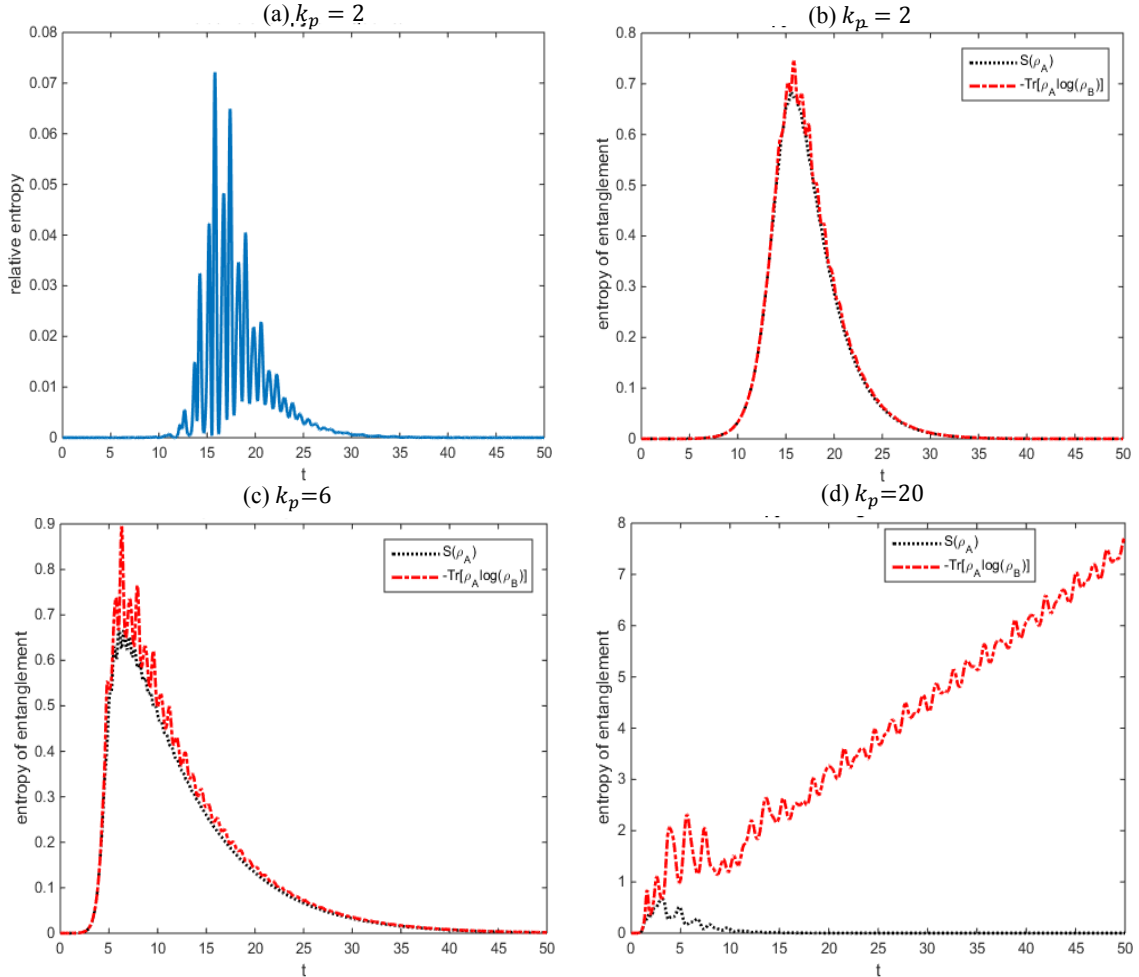


Fig. 6 Part (a) illustrates the time responses of the quantum relative entropy $S(\rho_A||\rho_B)$ in the qubit transfer process from $|00\rangle$ to $|11\rangle$. Parts (b), (c), and (d) are the comparison of $S(\rho_A)$ (black line) with $-\text{Trace}(\rho_A \log_2 \rho_B)$ (red line) for $k_p = 2$, $k_p = 6$ and $k_p = 20$, respectively.

5.4 Concurrence

Different from the former three indices of entanglement, the concurrence [21] is a quantification of two-electron correlation without using Schmidt decomposition. This quantity is defined for pure states and can be calculated analytically as

$$C(\rho) = \max\{0, \lambda_1 - \lambda_2 - \lambda_3 - \lambda_4\} \quad (5.9)$$

where, λ_i , $i = 1, 2, 3, 4$, are the decreasingly ordered eigenvalues of the matrix

$$R = \sqrt{\sqrt{\rho}(\sigma_y \otimes \sigma_y)\rho^*(\sigma_y \otimes \sigma_y)\sqrt{\rho}} \quad (5.10)$$

and σ_y is the Pauli-Y matrix defined in Eq. (2.9). The concurrence falls in the interval $0 \leq C(\rho) \leq 1$, with $C(\rho) = 0$ corresponding to the separable state and $C(\rho) = 1$ to the maximally entangled state. By substituting the density matrix $\rho(t)$ computed by Eq. (4.4), the concurrence $C(\rho(t))$ can be expressed as a function of time t and the result is plotted in Fig. 7 for the qubit transfer process from $|00\rangle$ to $|11\rangle$ with two different control gains $k_p = 2$ and $k_p = 20$. It is found that the time response of $C(\rho(t))$ increases initially from zero, then achieves its maximum in the middle of the transition and decays to zero at the end of transition process. The comparison between Figs. 5 and 7 demonstrates the similarity of $C(\rho(t))$ with the

entanglement entropy $E(\psi(t))$. Both the indices indicate that high-gain control leads to an unsteady and oscillatory entanglement between the two electrons.

Another useful index of entanglement is the entanglement of formation $E_F(\rho)$ [22], which can be expressed in terms of the concurrence as

$$E_F(\rho) = H\left(\frac{1 + \sqrt{1 - C^2(\rho)}}{2}\right) \quad (5.11)$$

where, $H(x) = -x \log x - (1 - x) \log(1 - x)$ is the binary entropy function. Like the concurrence $C(\rho)$, the entanglement of formation falls in the interval $0 \leq E_F(\rho) \leq 1$, with $E_F(\rho) = 0$ corresponding to the separable state and $C(\rho) = 1$ to the maximal entangled state. The resulting time response of $E_F(\rho(t))$ has a high degree of similarity with $C(\rho(t))$ and its illustration is omitted here.

6. Qubit Transfer via Intermediate Entangled States

From the time responses of the several quantitative measures of entanglement mentioned above, it is evident that increasing the degree of entanglement during the qubit transfer process is helpful to improve the convergence to the target state. The lack of sufficient

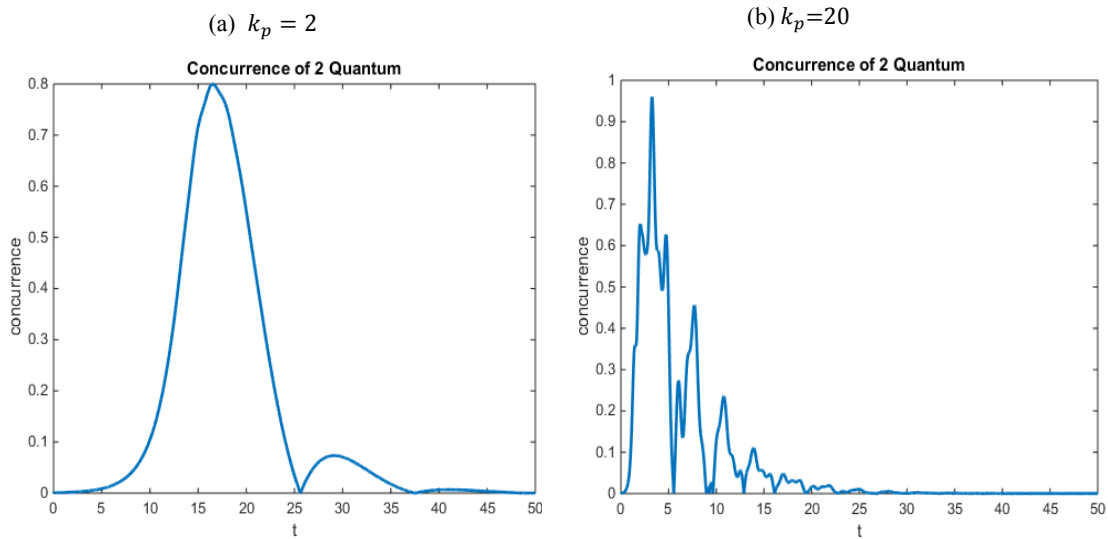


Fig. 7 The concurrence $C(\rho(t))$ is plotted as a function of time t for the qubit transfer process from $|00\rangle$ to $|11\rangle$ with two control gains $k_p = 2$ and $k_p = 20$.

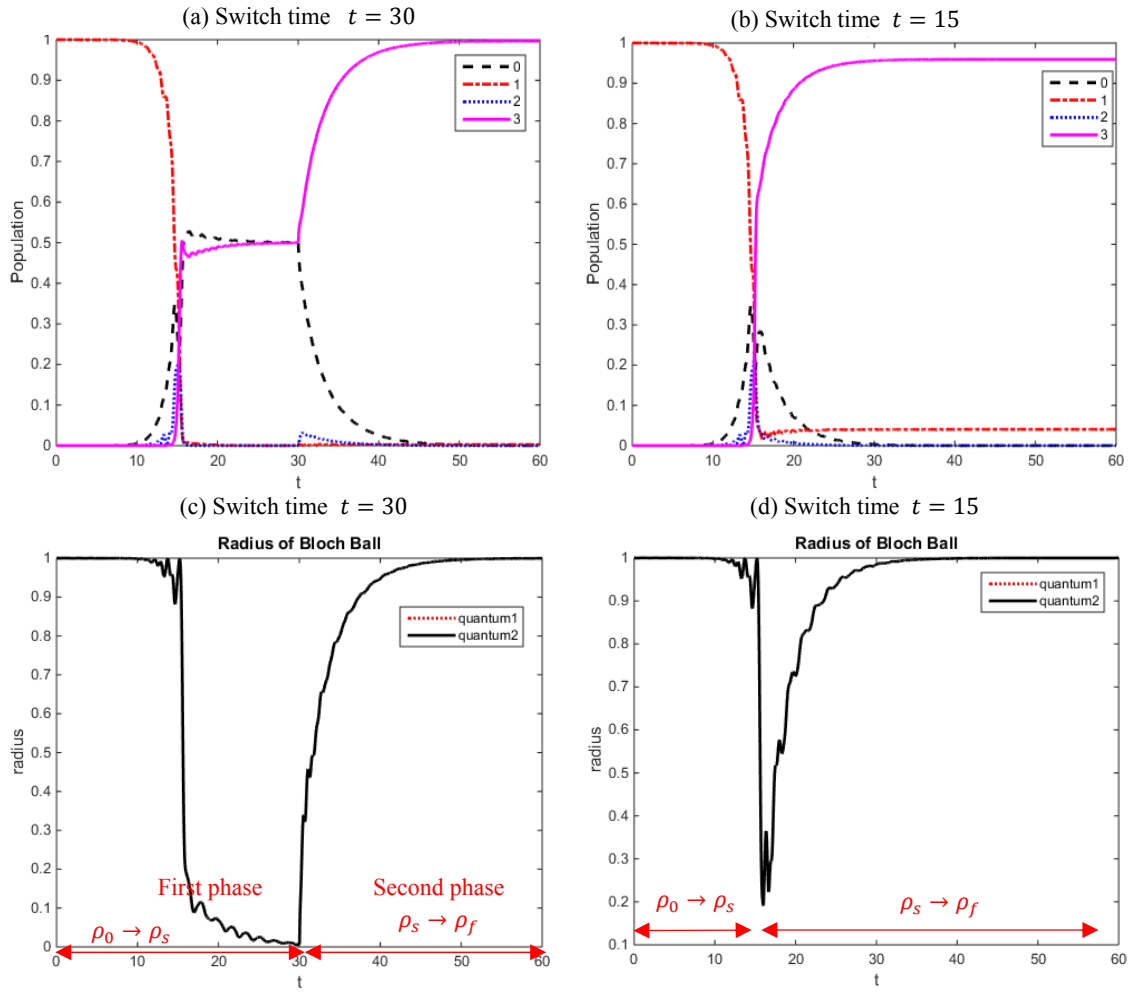


Fig. 8 The qubit transfer from $\rho_0 = |01\rangle$ to $\rho_f = |11\rangle$ via the intermediate entangled state $\rho_s = (|00\rangle + |11\rangle)/\sqrt{2}$. Parts (a) and (b) show the transition process by using two different switch times from the first phase $\rho_0 \rightarrow \rho_s$ to the second phase $\rho_s \rightarrow \rho_f$. Parts (c) and (d) are the corresponding time responses of the Bloch radius.

quantum correlation between the initial and final qubits is the main reason for unavailable transfer between them. This observation motivates us to insert an intermediate entangled state into a transition process between two qubits for which direct transfer between them is not possible. A similar strategy called path programming [28] was used in energy-level transfer control, where several intermediate states are selected as the transitional target states to form a transition path connecting the initial and terminal states between which direct transfer is unavailable by Lyapunov control. Due to the additional quantum correlation established by entanglement, which is otherwise absent in energy-level transfer control, the use of an intermediate state in multi-qubit transfer

control is expected to be more effective than that used in energy-level transfer control.

Between the given initial state ρ_0 and final state ρ_f , the insertion of an intermediate entangled state ρ_s divides the process into two parts:

$$\rho_0 \xrightarrow{1} \rho_s \xrightarrow{2} \rho_f \quad (6.1)$$

For the first part $\rho_0 \rightarrow \rho_s$, the target state is ρ_s and accordingly, the observable operator defined in Eq. (3.6) can be chosen as

$$P^{(1)} - \rho_s \quad (6.2)$$

The related control law $u^{(1)}$ given by Eq. (3.5) is designed to transfer the system state from ρ_0 to ρ_s . For the second part $\rho_s \rightarrow \rho_f$, the target state is ρ_f and the observable operator is chosen as

$$P^{(2)} = -\rho_f \quad (6.3)$$

The related control law $u^{(2)}$ is designed to transfer the system state from ρ_s to ρ_f . The intermediate entangled state ρ_s plays the role of an information medium via which information is exchanged between ρ_0 and ρ_f so as to strengthen their correlation and facilitate the qubit transfer between them.

The necessity of inserting an intermediate entangled state is demonstrated in the qubit transfer from $|01\rangle$ to $|11\rangle$, between which direct transfer is unattainable by the Lyapunov control law of Eq. (3.5). If the Bell state $(|00\rangle + |11\rangle)/\sqrt{2}$, a maximally entangled state, is chosen as the intermediate entangled state ρ_s , the qubit transfer can be realized easily via the transition process $\rho_0 \rightarrow \rho_s \rightarrow \rho_f$. As shown in Fig. 8a, during the first transition $\rho_0 \rightarrow \rho_s$, the Bell state ρ_s is reached at $t_s = 30$, after which the second transition $\rho_s \rightarrow \rho_f$ is initiated and the terminal state $\rho_f = |11\rangle\langle 11|$ is attained at $t_s = 60$. The role of the intermediate entangled state ρ_s is crucial to the success of the qubit transfer and the choice of the transition switch time $t_s = 30$ is to ensure that the entangled state ρ_s is fully developed before starting the second transition $\rho_s \rightarrow \rho_f$.

To examine the influence of the intermediate entangled state ρ_s on the accuracy of the qubit transfer, we change the transition switch time from $t_s = 30$ to $t_s = 15$, at which the Bell state ρ_s is not fully developed in the first transition $\rho_0 \rightarrow \rho_s$. The entire transition process $\rho_0 \rightarrow \rho_s \rightarrow \rho_f$ via this premature intermediate state is shown in Fig. 8b. The resulting qubit transfer response is found to converge to a superposed state $0.0133|01\rangle + 0.9867|11\rangle$ instead of the expected state $|11\rangle$. Figs. 8c and 8d compare the time responses of the Bloch-ball radius for the two different switch times $t_s = 30$ and $t_s = 15$. In the case of $t_s = 30$, the minimal radius is zero, indicating that the Bell state is fully attained; while in the case of $t_s = 15$, the minimal radius is 0.1908, corresponding to a premature Bell state. If the transition switch time t_s is reduced further, the qubit

transfer error gets larger and eventually diverges just like the direct-transfer situation without an intermediate entangled state.

7. Conclusions

Quantum entanglement is omnipresent throughout a qubit transfer process, even though both the initial and final states are not entangled states. Several indices of entanglement have been employed in this paper to evaluate the qubit transfer performance for a two-qubit system composed of two spin-coupled electrons. By inspecting the transient responses of the various indices of entanglement, we find that the accuracy of qubit transfer strongly depends on the degree of entanglement that can be achieved during the transition process, and the degree of entanglement is in turn determined by the imposed qubit control law. The comparison of low-gain and high-gain Lyapunov control shows that quantum entanglement is vulnerable to strong field and a high-gain control tends to attenuate the degree of entanglement and reduce the accuracy of qubit transfer. Our results show that the indices of entanglement, especially quantum relative entropy, can be served as a useful cost function to evaluate the performance of qubit control. On the other hand, for quantum systems lacking for sufficient quantum correlation between the states to be transferred, the insertion of an intermediate entangled state into the transition process helps to connect the two qubits by increasing the entanglement between them.

References

- [1] Bennett, C. H., Brassard, G., Crepeau, C., et al., 1993. "Teleporting an Unknown Quantum State via Dual Classical and Einstein-Podolsky-Rosen Channels." *Physical Review Letters* 70: 1895-9.
- [2] Nielsen, M. A., and Chuang, I. L. 2010. *Quantum Computation and Quantum Information*. Cambridge: Cambridge University Press.
- [3] Ekert, A. K. 1991. "Quantum Cryptography Based on Bells Theorem." *Physical Review Letters* 67: 661-3.
- [4] Bennett, C. H., and Wiesner, S. J. 1992. "Communication via One- and Two-particle Operators on

- Einstein-Podolsky-Rosen States.” *Physical Review Letters* 69: 2881-4.
- [5] Dong, D., and Petersen, I. R. 2010. “Quantum Control Theory and Applications: A Survey.” *IET Control Theory and Applications* 4: 2651-71.
- [6] Kuang, S., and Cong, S. 2008. “Lyapunov Control Methods of Closed Quantum Systems.” *Automatica* 44: 98-108.
- [7] Cong, S., and Meng, F. F. 2013. “A Survey of Quantum Lyapunov Control Methods.” *The Scientific World Journal* 2013 (1): 967529.
- [8] Cong, S. 2014. *Control of Quantum Systems—Theory and Methods*. Singapore: John Wiley & Sons.
- [9] Wang, X., and Schirmer, S. G. 2010. “Analysis of Lyapunov Method for Control of Quantum States.” *IEEE Transactions on Automatic Control* 55: 2259-70.
- [10] Wang, X., and Schirmer, S. G. 2009. “Entanglement Generation between Distant Atoms by Lyapunov Control.” *Physical Review A* 80: 042305.
- [11] Wiseman, H. M. 1994. “Quantum Theory of Continuous Feedback.” *Physical Review A* 49: 2133-50.
- [12] Mabuchi, H., and Zoller, P. 1996. “Inversion of Quantum Jumps in Quantum Optical Systems under Continuous Observation.” *Physical Review Letters* 76: 3108-11.
- [13] Wang, J., Wiseman, H. M., and Milburn, G. J. 2005. “Dynamical Creation of Entanglement by Homodyne-Mediated Feedback.” *Physical Review A* 71: 042309.
- [14] Doherty, A. C., and Jacobs, K. 1999. “Feedback Control of Quantum Systems Using Continuous State Estimation.” *Physical Review A* 60: 2700-11.
- [15] Ruskov, R., and Korotkov, A. N. 2002. “Quantum Feedback Control of a Solid-State Qubit.” *Physical Review B* 66: 041401.
- [16] Hill, C., and Ralph, J. 2008. “Weak Measurement and Control of Entanglement Generation.” *Physical Review A* 77: 014305.
- [17] Hou, S. C., Khan, M. A., Yi, X. X., Dong, D., and Petersen, I. R. 2012. “Optimal Lyapunov-Based Quantum Control for Quantum Systems.” *Physical Review A* 86: 022321.
- [18] Wang, L. C., Hou, S. C., Yi, X. X., Dong, D., and Petersen, I. R. 2014. “Optimal Lyapunov Quantum Control of Two-Level Systems: Convergence and Extended Techniques.” *Physics Letters A* 378: 1074-80.
- [19] Ekert, A., and Peter, L. K. 1995. “Entangled Quantum System and the Schmidt Decomposition.” *American Journal of Physics* 63: 415-23.
- [20] Vedral, V., and Plenio, M. B. 1998. “Entanglement Measures and Purification Procedures.” *Physical Review A* 57: 1619-33.
- [21] Hill, S., and Wootters, W. K. 1997. “Entanglement of a Pair of Quantum Bits.” *Physical Review Letters* 78: 5022-5.
- [22] Bennett, C. H., Brassard, G., Popescu, S., et al. 1996. “Purification of Noisy Entanglement and Faithful Teleportation via Noisy Channels.” *Physical Review Letters* 76: 722-5.
- [23] Mirrahimi, M., Rouchon, P., and Turinici, G. 2005. “Lyapunov Control of Bilinear Schrödinger Equations.” *Automatica* 41: 1987-94.
- [24] Yang, F., and Cong, S. 2012. “Preparation of Entanglement States in a Two-Spin System by Lyapunov-Based Method.” *Journal of Systems Science and Complexity* 25: 451-62.
- [25] Beauchard, K., Coron, J. M., Mirrahimi, M., and Rouchon, P. 2007. “Implicit Lyapunov Control of Finite Dimensional Schrödinger Equations.” *Systems and Control Letters* 56: 388-95.
- [26] Zhao, S., Lin, H., Sun, J., and Xue, Z. 2012. “An Implicit Lyapunov Control for Finite-Dimensional Closed Quantum Systems.” *International Journal of Robust and Nonlinear Control* 22: 1212-28.
- [27] Ayman, F. A., Bahaa, E. A. S., Alexander, V. S., et al. 2001. “Degree of Entanglement for Two Qubits.” *Physical Review A* 64: 050101.
- [28] Lou, Y., Cong, S., Yang, J., and Kuang, S. 2011. “Path Programming Control Strategy of Quantum State Transfer.” *IET Control Theory and Applications* 5: 291-8.